KSCE Journal of Civil Engineering (2018) 22(2):747-754

DOI 10.1007/s12205-017-1433-9

Structural Engineering

pISSN 1226-7988, eISSN 1976-3808
www.springer.com/12205

The Effective Near-surface Defect Identification by Dynamic Behavior Associated with Both Impact-echo and Flexural Modes for Concrete Structures

Inbok Lee*, Seung-Hee Kwon, Jongil Park***, and Taekeun Oh******

Received September 1, 2016/Revised January 12, 2017/Accepted February 13, 2017/Published Online March 22, 2017

Abstract

The Impact Echo (IE) test is a robust Non-destructive Test (NDT) method where the dynamic response of a target area results from an impact event to make decisions about the damage identification of concrete structures. However, the IE data over the near-surface delamination typically developed by rebar corrosion at the cover depth is not easy in interpreting because of the difficulties in the dynamic analysis of flexural modes over the defects as well as in the identification of weak and unclear signal of the high IE frequency corresponding to the delamination depth. The shallow delamination in the concrete structures must be clearly identified and interpreted such that infrastructure engineers can effectively check the condition of the structure. To address this problem, we proposed the combined dynamic characterization with both impact-echo and flexural modes in order to identify the area and degree of damage and applied this technique to the designated concrete slab and the simulated bridge deck with various artificial defects at the depth of rebar. The test results proved that the imaging technique by the combined mode associated with the IE and flexural modes is more effective and accurate for the detection of shallow defects in the concrete slab than one by the individual mode.

Keywords: *concrete, impact-echo mode, flexural mode, non-destructive testing, damage identification, shallow delamination, near-surface defect*

1. Introduction

The deterioration of reinforced or prestressed concrete structures due to corrosion of rebar or tendon as well as the aging has been critical issues that will require great attentions by governments and public to ensure the safety (Hime and Erlin, 1987; Gannon and Cady, 1992). Especially, various near-surface defects of concrete slabs, bridge deck, and pavements mainly due to the corrosion and the direct external force such as the traffic load are a matter of grave concern because large costs for repair and rehabilitation should be allocated according to severity and risk of the structures. Although the condition evaluation of the near-surface defects is investigated typically by visual inspection and restricted core sampling, a few of classical Non-destructive Test (NDT) methods such as the hammering inspection and infrared thermography have been proposed to check and confirm such defects within concrete structures. For example a hammering inspection has been popularly applied to monitor shallow delaminations in concrete slabs or pavements. However, such sounding method can take a long time for the test and measurement and the analysis results may depend on an inspector's skill and experience (Fuchs and Washer, 2004). As another example, infrared thermography has been used to detect the near-surface defects, but it is also dependent on the environmental factors such as temperature and humidity (Oh *et al.,* 2012). Thus, investigation of shallow-depth defects can be time-consuming and subjective and often requires a variety of devices and advanced methods to draw consistent and reliable conclusions (Moore *et al*., 2001; Huston *et al.*, 2007)

One of the effective NDT methods for the integrity assessment is the Impact Echo (IE) test based on the seismic characterization (Sansalone and Streett, 1997). In the IE test, a low frequency mechanical wave source is applied to a target structure, and the resulting dynamic behavior is observed. The response is interpreted in the frequency domain in order to identify resonance frequencies; flexural and thickness stretch modes. The IE test which is usually focused on the thickness stretch mode (e.g. IE mode) in concrete structures enables estimation of slab thickness as well as identification of the planar defects (Oh *et al.,* 2013a). A lot of approaches on the basis of the IE method have been implemented to handle the effective presentation of NDT data for various concrete structures (Buyukozturk, 1998). Liu and Yiu (2002) proposed the spectral B- and C-scan images to represent surface-opening and internal cracks. Schubert *et al.* (2004) used the

*Member, Adjunct Professor, Environment Technology and Safety Technology Convergence, Inha University, Incheon 22201, Korea (E-mail: pposic10@naver.com)
**Member, Associate Professor, Dept. of Civil and Environmental Engineering, Myongji University, Yongin 17058, Korea (E-mail: kwon08@mju.ac.kr)
***Associate Professor, Dept. of Safety Engineering, Seoul National University of Science and Technology, Seoul 01811, Korea (E-mail: jip111@seoultech.ac.kr)
****Associate Professor, Dept. of Safety Engineering, Incheon National University, Incheon 22012, Korea (Corresponding Author, E-mail: tkoh@inu.ac.kr)

spectral B-scan image to measure the thickness of concrete specimens.

However, these approaches have focused only on the impact-echo mode. As mentioned above, the flexural mode identified by the natural frequencies of a structure and the modal properties can be also used for the effective characterization of concrete defects such as near-surface delaminations by the corrosion at the cover depth. For the excitation of each mode, the proper size of impact hammer and the sensor with the adequate frequency range should be selected because the dominant frequency ranges of the impact-echo and flexural modes, respectively are usually different. For example, the IE frequency corresponding to the shallow delamination at the 40 mm depth is about 48 kHz and the hammer size for the excitation of the frequency should be less than 6 mm based on the Hertz theory (Johnson, 1985). However, the 6 mm hammer size is not appropriate for the excitation of the flexural mode with the typical range of 0 ~ 6 kHz as well as the IE mode with the range of 6 ~ 12 kHz corresponding to the range of the 150-300 mm slab thickness (Sansalone and Streett, 1997). Thus, the repetitive

IE tests over the same test point changing the size of impact-hammer and the type of sensor has been performed for the excitation of the target mode, which makes the IE test uneasy and annoying. To address this problem, we used both the IE mode over the solid region and the flexural mode over the near-surface delamination with the one set of the impact-hammer and the sensor. Thus, this study proves that the imaging technique by both the impact-echo and the flexural modes can provide a better characterization of defects only by one test set-up without changing the size of impact-hammer and the type of sensor.

2. Air-coupled Impact-echo Method

The IE method is comprised of a contact sensor (usually displacement sensor), an impactor, a data acquisition and a computer. The obtained response signals by physically touching the surface of the target concrete structures are transformed into the frequency domain, for example using a Fast Fourier Transform (FFT) protocol, and dominant vibrational responses are identified in the frequency spectrum (amplitude) as spectral peaks. Two different types of dynamic behavior are usually expected: the flexural mode over delaminated region and thickness mode over solid (sound) region. Generally the modal frequencies associated with the flexural modes are significantly lower than those with the thickness modes, so occurrences of dominant low frequency modes are associated with the presence of delamination underneath and nearby the region of the test point.

Concrete infrastructures such as slab, bridge deck and pavement structures tend to be massive, with a large area to be inspected. A thorough examination of the infrastructures using a set of individual point tests across the structure area requires an enormous amount of tests and time to carry them out. To solve this issue, air-coupled sensing has been recently implemented. In air-coupled IE testing the conventional contact sensor is replaced with a contactless (air-coupled) sensor. The basis of air-coupled sensing is that leaky waves propagate into the air that bounds the concrete deck, caused by the generated wave motion of the surface (Zhu and Popovics, 2001). Although the amplitudes of these leaky waves are very small, air-coupled sensors can detect these leaky wave components with excellent fidelity and high signal to noise ratio. In fact properly configured air-coupled sensors provide equivalent IE data as that collected using conventional contact sensors (Zhu and Popovics 2007).

On the other hand, the flexural modes over shallow or mid-depth delaminations are more dominant than the IE modes, so the flexural mode can be used for the effective damage detection. For the better understanding, typical IE data in the time and frequency domain over sound and near-surface defect area, respectively, in a concrete bridge deck are presented in Fig. 1. In the sound region, the dynamic behavior is dominated by the stretch mode (IE mode), which shows that the resonance peak is observed at approximately 7.8 kHz, corresponding to the 250 mm depth in Fig. 1(b). However, the bending (flexural) modes is much more dominant over shallow delamination. These modes have fundamentally

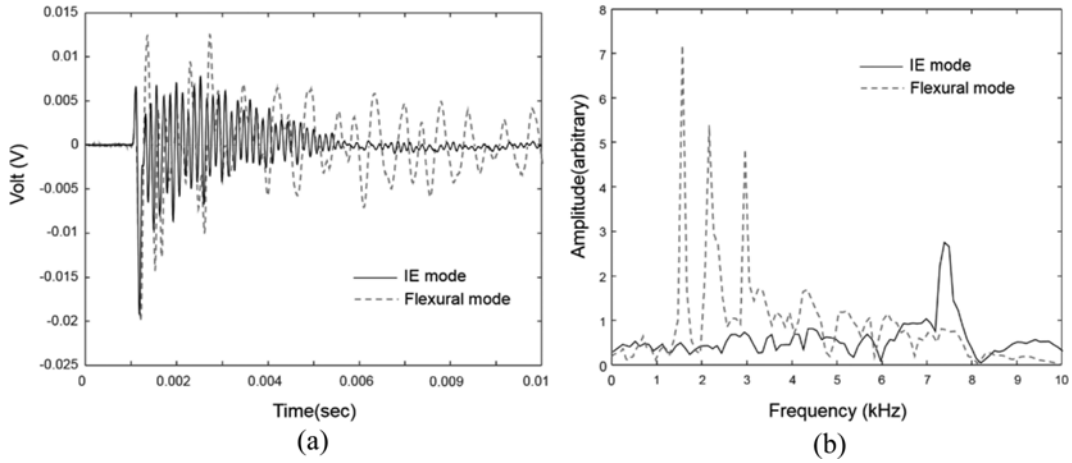

Fig. 1. Typical IE Data Tested Over Sound and Near-surface Defect Area: (a) Time Domain, (b) Frequency Domain

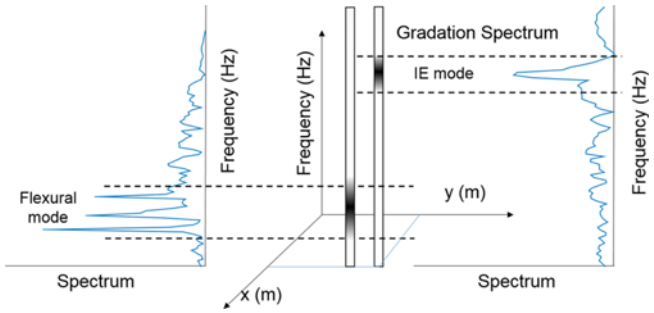

Fig. 2. Illustration of a Typical Pattern of Line Spectra Over a Shallow Delamination and a Solid Region. The Dark Shading Presents the High Spectral Amplitude

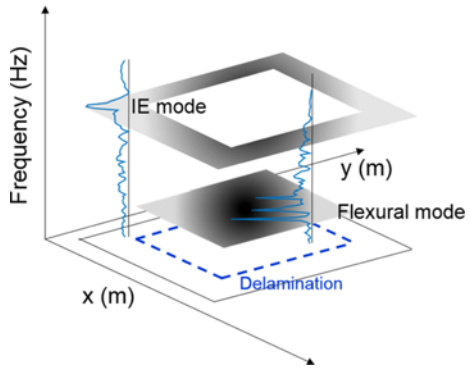

Fig. 3. Illustration of Spectral Amplitude IE Data Obtained Over a Shallow Delamination: The Dashed Line Shows the Delamination Area. The Dark Shading Presents the High Spectral Amplitude

different mode shapes and usually occur at lower frequencies (0 ~ 6 kHz) than the thickness stretch mode (Oh and Popovics, 2015a). Thus, this study proposes the imaging technique by the combined mode using both the IE and flexural modes.

The line spectrum is represented by an A-scan data over an IE test point. The characteristics of line spectra over a shallow delamination and solid regions, respectively are different, as illustrated in Fig. 2. The IE data over a shallow delamination have the larger dominant peaks in the lower frequency range than ones over a solid region. Also, a series of individual spectra over the test area space can make a volume data, as illustrated in Fig. 3. A XY plane at a frequency is defined to be a "C-scan". The volume plot contains all the data over both sound and defect area, but the internal data are hidden by the opacity of the surface data. However, the inside volume data can come into the view only by selecting a data sub-set of interest. Within a specific frequency region, usually between two frequency values, the flexural characteristics over the delamination are only presented by screening out the unnecessary parts of the volume data. This is approached by setting-up a certain value (a cut-off frequency) including fundamental natural modes above near-surface plate defects. The plan view of the volume plot displays the distinct amplitudes in a visible contour for the accurate detection of the defect region (Oh and Popovics, 2015a). However, the volume plot needs a lot of memory and storage for the computation because all the data are contained throughout the process. A more efficient imaging process can be achieved by data squeezing and compression, where all the data stacked between two predefined frequencies in a XY plane are deducted to provide a plan view image that is equivalent to that of the volume plot. We can accumulate all the spectral amplitudes through frequency at each gradation spectrum, map those summation across test area, and then normalize with respect to maximum within data volume, providing a "stacked C-scan. The stacked C-scan data are mapped across all x-y test locations that represent the test surface; stacked C-scan plots define the region of near-surface defect well (Oh and Popovics, 2015b).

On the other hand, the thickness stretch vibration mode (IE mode) can be implemented to complement the flexural mode behavior captured with the stacked C-scan image, for improved defect characterization. The IE modes corresponding to various depths of delaminations can be identified by selecting the appropriate size of an impactor and the sensitivity of a sensor. However, it is not feasible to examine a massive deck structure using changing testing set-ups, as that would require an enormous amount of effort and time to carry out. Rather, one data set obtained with the consistent testing set-up without the change of impactor and sensor is preferred, as long as the single size of ball impactor and sensor can effectively excite the flexural and thickness modes of interest. In this way, the solid region can be differentiated from a defect region only by representing the amplitude spectrum at the IE frequency corresponding to the slab depth which can be known in advance.

This study combines the behavior of flexural modes over defect region, indicated by stacked C-scan images, and that of the IE thickness mode over solid region by the amplitude spectrum at IE frequency. The combined image is obtained by subtracting the IE response image from the stacked C-scan image, pixel by pixel. The effectiveness for defect characterization is investigated by applying the combination technique in experiments on concrete samples that contain delamination defects.

3. Experiments with Controlled Delaminations

3.1 Test Specimens

To investigate the effectiveness of combine imaging technique with the stacked C-scan and IE mode to characterize shallow delaminations in concrete structures, air-coupled IE tests were performed on a designated concrete slab and a simulated bridge deck built in the lab. The two specimens contain various artificial near-surface defects (shallow delaminations). Detail about the two test samples are presented in Fig. 4 and 5. The 28-day compressive strengths of all specimens are in the range of 30 to 40 MPa.

The dimension of the designated concrete slab is 1500 mm × 2000 mm × 250 mm (width × length × thickness). Fig. 4 shows a top view of the test slab. The test slab has rebars in two directions at two layers, 60 and 200 mm depths. The artificial planar defects (delaminations) and voids with a variety of size are embedded at

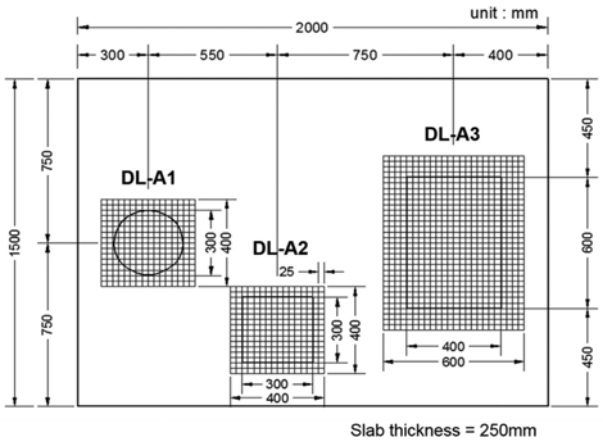

Fig. 4. A top view of Concrete Test Slab with the Dimension of 1500 mm (width)× 2000 mm (length) × 250 mm (thickness), Presenting the Size and Position of the Defects and the Test Grid Spacing with 25 mm in Both Directions

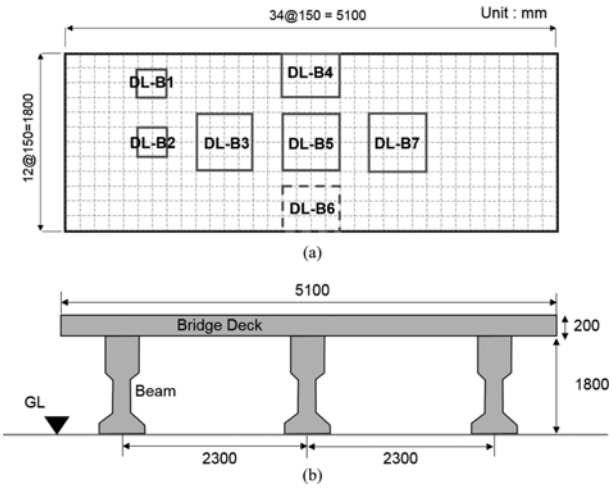

Fig. 5. Simulated Bridge Deck Specimen: (a) Plan View of the Specimen Showing the Location of the Defects and thE Test Grid Designation, (b) Section View of the Specimen; the Nominal Test Grid Spacing is 150 mm in Both Directions and the Clear Span of the Bridge is 1800 mm

various depths, as shown in Fig. 4 and Table 1. Two-layered plastic sheets with air voids and soft foam blocks were used for the simulation of square, rectangular and circular delaminations. The air-coupled tests were performed at the predefined 25 mm × 25 mm test grid

The simulated bridge deck (5100 mm (length) × 1800 mm (width) × 200 mm (depth)) is supported by three girders and was reinforced with two layers of rebar at 65 and 150 mm depths, respectively. The deck contained fabricated delaminations with various sizes and at 65 mm and 150 mm also by inserting double-layered plastic sheets. The locations and information of all the simulated defects in the test bridge deck are shown in Fig. 5 and Table 2. Although the 60 and 65mm cover depth in the architecture can be relatively large, it is reasonable for the reinforced slab or wall with more than 16 mm diameter rebar (D16) as well as for the foundation in the civil engineering.

3.2 Test Procedure

The consistent IE tests were set-up and carried out to the designated concrete slab and the simulated bridge deck with the different test grid. An impact ball hammer with an 18 mm diameter was applied to the two specimens. The input energy (forcing function) by the ball impactor presents stable and consistent frequency range up to 15 kHz. The dynamic behavior over the surface was measured by an air-coupled sensor which is a dynamic vocal microphone with the 1.85 mV/Pa sensitivity at 1 kHz and the operation frequency range of 50 Hz to 15 kHz. The air-coupled sensor is linked to the DAQ (data acquisition device), converting the analog data to digital one with a sampling rate of 1 MHz. The testing set-up is presented in Figure 6; the manual impact is applied nearby the air-coupled sensor and both the impactor and the sensor are moved together with a close and constant distance on a testing grid.

For each test, time signals with 8 ms duration are collected. All the time-domain data were normalized in respect of the negative

Table 1. Detailed Information of Preplaced Delamination Defects Within the Concrete Test Slab

Delamination	Width(mm)	Length(mm)	Depth(mm)	Delamination type
DL-A1	300 (Diameter)		60	Soft form with 50mm thickness
DL-A2	300	300	60	Double layered plastic sheets with 2mm thickness
DL-A3	400	600	60	Double layered plastic sheets with 2mm thickness

Table 2. Detailed Information of Preplaced Delamination Defects within the Simulated Bridge Deck

Delamination	Width (mm)	Length (mm)	Depth (mm)	Delamination type
DL-B1	300	300	65	Thin form with 2mm thickness
DL-B2	300	300	65	Thin form with 1mm thickness
DL-B3	600	600	65	Thin form with 1mm thickness
DL-B4	600	450	65	Thin form with 2mm thickness
DL-B5	600	600	65	Thin form with 2mm thickness
DL-B6	600	450	150	Thin form with 1mm thickness
DL-B7	600	600	65	Thin form with 2mm thickness

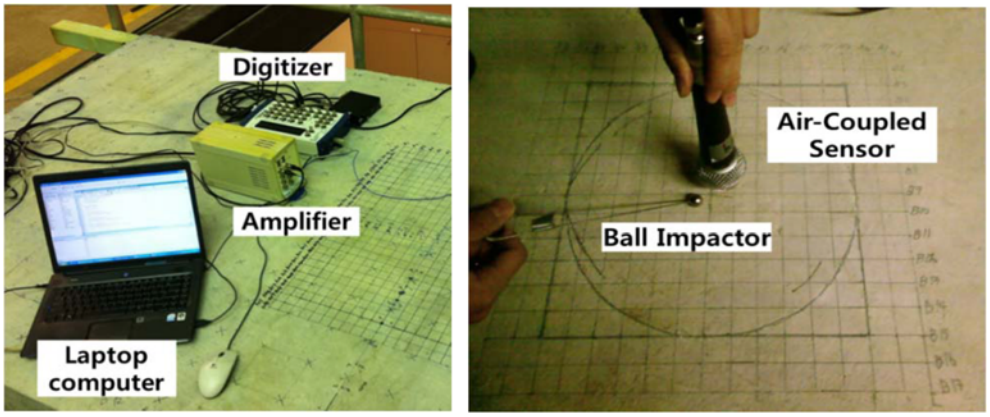

Fig. 6. The Air-coupled IE Test Set-up: (a) Data Acquisition System, (b) Impactor and Air-coupled Sensor Set

peak of the Rayleigh (surface) wave for the application of the consistent impact energy. The normalized time signals are transferred and stored on the computer associated with the DAQ system for a next process. The collected test data are transformed to the amplitude spectra in the frequency-domain by Fast Fourier Transformation (FFT).

We assumed that the position and depth of defects are unknown, but that the depth of the slab (250 mm) is known in advance because the dimension of structures can be typically accessed by the design drawing, visual inspection, and other NDE methods such as the ultrasonic and IE method.

First, the spectral amplitude plot at the IE mode frequency (7.8 kHz) corresponding to the depth of the slab (250 mm) was created to identify the solid region out of the delamination area because the IE frequency of the slab depth does not dominate over shallow delaminations. Second, regarding the flexural mode, the high spectral amplitudes in the low-frequency range dominated over shallow defects. For the effective imaging process by the flexural modes over the shallow delaminations, the stacked C-scan up to 5 kHz was used. For typical shallow delamination defects with a range of areal dimensions (0-2000 mm) and depths (0-100 mm), the first few flexural frequencies are within 0 ~ 6 kHz on the basis of the plate vibration theory with a semi-clamped boundary condition (Oh *et al.*, 2013b). Lastly, the combined imaging technique associated with both the spectral amplitudes at the IE frequency and the stacked C-scan images by the flexural modes were implemented for the better defect characterization.

4. Results and Discussion

The combined imaging technique, using the stacked C-scan image by the flexural modes and the amplitude spectrum by IE mode, is applied to all the data sets collected from the concrete test slab and the simulated bridge deck. The image processing is implemented using the MATLAB contour plot. Also, the C-scan images from the flexural and IE modes, respectively were presented for the comparison with one from the combined imaging technique.

The C-scan images for the flexural modes were stocked up to 5 kHz in a single plane. These image plots are presented in Figs. 7(a), 8(a), 9(a) and 10(a) and show good performance for defect size detection except for the near-boundary regions because the first few low-order modes up to 5 kHz have the low amplitude for the mode shape nearby the boundary. The contour plot of the spectral amplitude at the IE frequency are given in Figs. 7(b),

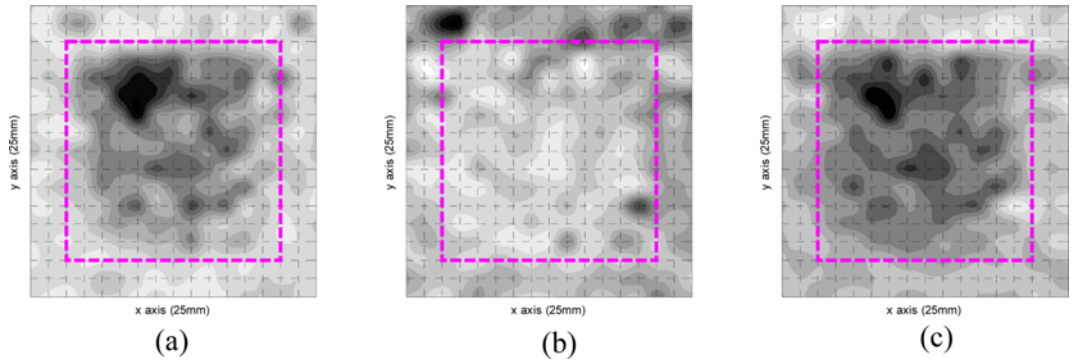

Fig. 7. Contour Plot Representation of the Spectral Amplitude Data for the Square Delamination: (a) The Stacked C-scan Image (0~5 kHz), (b) Spectral Amplitudes at the IE Frequency (7.8 kHz), (c) the Stacked C-scan Images with thE Removed Spectral Amplitudes at the IE Frequency; the Dashed Line Presents the Delamination Boundary

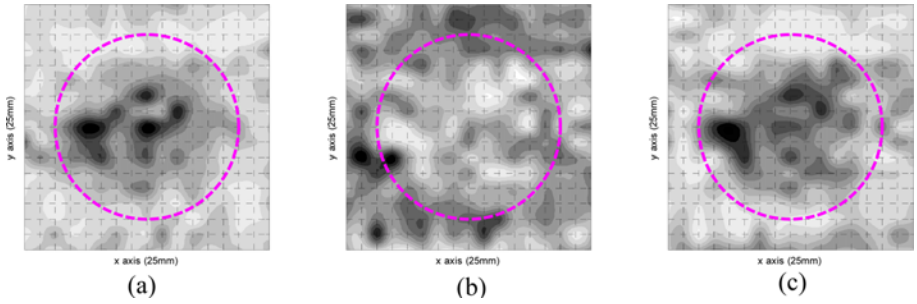

Fig. 8. Contour Plot Representation of the Spectral Amplitude Data for the Circle Delamination: (a) the Stacked C-scan Image (0~5 kHz); (b) Spectral Amplitudes at the IE Frequency (7.8 kHz), (c) the Stacked C-scan Images with the Removed Spectral Amplitudes at the IE frequency; the Dashed Line Presents the Delamination Boundary

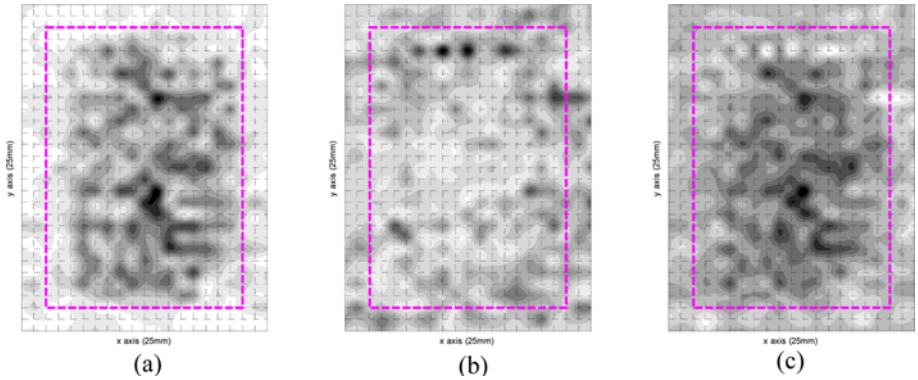

Fig. 9. Contour Plot Representation of the Spectral Amplitude Data for the Rectangular Delamination: (a) the Stacked C-scan Image (0~5 kHz), (b) Spectral Amplitudes at the IE Frequency (7.8 kHz), (c) the Stacked C-scan Images with the Removed Spectral Amplitudes at the IE Frequency the Dashed Line Presents the Delamination Boundary

8(b), 9(b) and 10(b). The spectral plot shows some noise regardless of the boundary, especially over the rectangular defect (Fig. 9(b)). Although it may happen by the partial fabrication error with regard to the artificial defect, the cause is likely from interfacial defect contact caused by the impact event. Also, in many test points, the differences between the spectral amplitudes of the IE frequency and others are minor, which can make the noise beyond defect boundary. However, the combined flexural and IE plots (Figs. 7(c), 8(c), 9(c), and 10(c)) define more accurate areas of shallow delaminations than the imaging presentation by the flexural and IE modes, respectively. Absolutely, the defect estimation nearby boundary is much improved and the noise out of defect area is minimized because each mode makes up for the mutual weakness.

If the test grid is comparatively wider, as shown in Fig. 10, small size defects cannot be covered, irrespective of other performance factors. Furthermore, if the cut-off frequency value is too low, flexural vibration behavior of the smaller or deeper defects will not be found, because the frequency range is out of our expected one. If the sizes and depths of the defects are beyond the defined range, the cut-off frequency should be changed accordingly.

For the quantitative comparison, the comparative accuracies among all the imaging plots by flexural, IE, and combined mode were calculated. For the analysis of each image, a binary map (yes or no) is completed, where the threshold for the determination of the defect or no defect is changed until obtaining an optimum

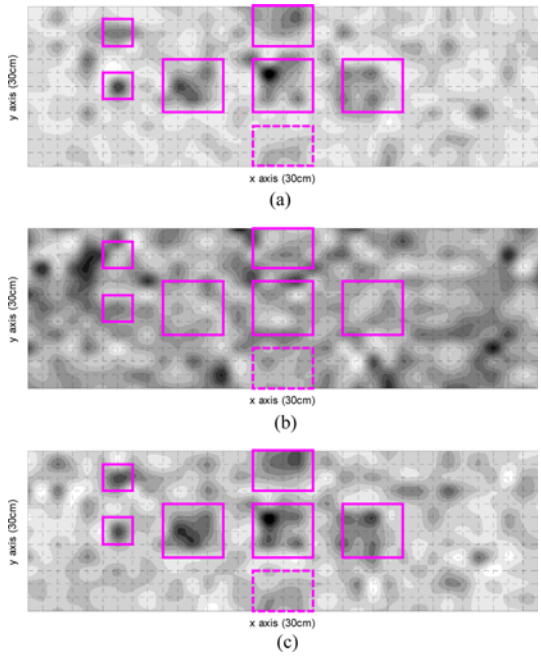

Fig. 10. Contour Plot Representation of the Spectral Amplitude Data for the Simulate Bridge Deck: (a) the Stacked C-scan Image (0~5 kHz), (b) Spectral Amplitudes at the IE Frequency (9.6 kHz), (c) the Stacked C-scan Images with the removed Spectral Amplitudes at the IE Frequency; the Pink Solid and Dashed Lines Indicate Delamination Boundaries with the 65 mm and 150 mm Depths, Respectively.

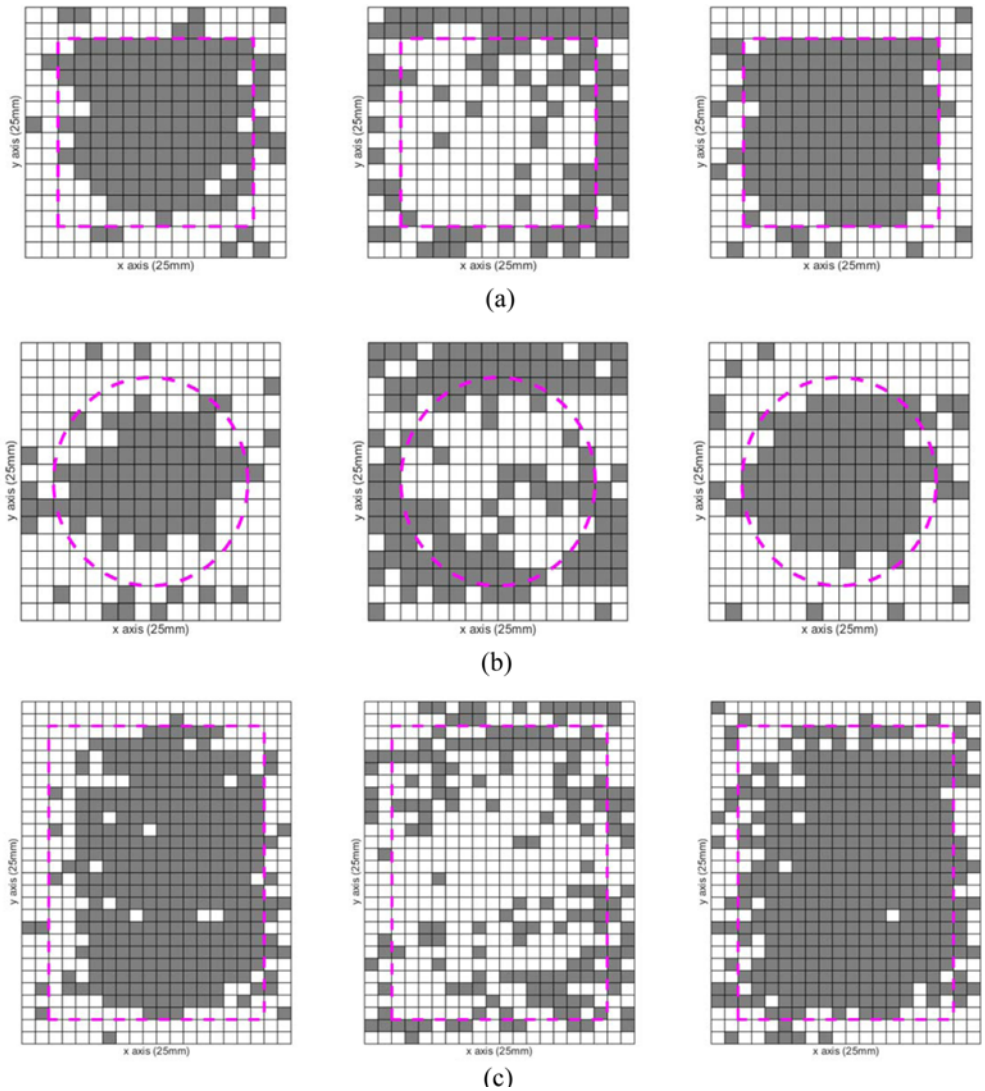

Fig. 11. Presentation of Binary Maps Implemented by Optimum Threshold Values for: (a) Square, (b) Circle, (c) Rectangular Delaminations; Each Binary Map Shows the Stacked C-Scan Image(left), Spectral Amplitudes at the IE Frequency (middle), the Stacked C-scan Images with the Removed Spectral Amplitudes at the IE Frequency (right)

Table 3. Relative Accuracy and Noise of the Imaging by Flexural, IE and, Combined Modes

Delamination	Flexural mode		IE mode		Combined mode	
	In delamination (Accuracy)	Out of delamination (Noise)	In delamination (Accuracy)	Out of delamination (Noise)	In delamination (Accuracy)	Out of delamination (Noise)
Square	81.25%	18.75%	78.47%	34.82%	91.67%	16.07%
	Threshold = 21%		Threshold = 28%		Threshold = 45%	
Circle	67.31%	12.50%	41.35%	58.55%	84.62%	11.84%
	Threshold = 25%		Threshold = 31%		Threshold = 51%	
Rectangular	66.90%	15.63%	25.93%	89.84%	75.46%	21.88%
	Threshold = 22%		Threshold = 27%		Threshold = 48%	

match to predefined boundary region with the minimum error out of the boundary. The plot accuracy is presented by percentage of agreement degree within the defined defect region with regard to all the image pixels. The noise out of the defect area is also calculated as percentage of incorrect prediction beyond the defect region. Each threshold value was determined by iterative process for the optimization with both the best match in the defect boundary and the minimum noise out of the region. The resulting binary images of the square, circular, and rectangular shallow defects are presented in Fig. 11.

The comparative accuracies from the analysis are summarized in Table 3. The results indicate that the imaging plots by the

combined mode presents the best accuracy regardless of a type of delamination, with minimum noise compared to ones by the flexural and IE modes. The spectral amplitudes map at the IE frequency shows poorest, but still acceptable. The accuracy of the imaging plot by the flexural mode is equivalent to, although moderately lower than, that for the image by the combined modes for all three defects. However, the slab depth for the imaging technique by the combined mode must be known in advance, whereas this information is not needed for the imaging technique by flexural mode within the designated cutoff frequency.

Impact-echo testing has been highly successful in locating and evaluating the near-surface defects and has clearly exited both the IE and flexural modes (Sansalone and Streett, 1997). However, the improper field application of impact-echo such as an inefficient testing set-up and an erroneous interpretation may be unsuccessful in the identification of defects. In this regard, the field application of the proposed method can complement and strength the accuracy and reliability of IE data by using the IE and flexural modes together, but the field engineers should know the dynamic behavior of the target structure and the embedded defects in advance.

5. Conclusions

We propose an imaging technique by the combined mode associated with the flexural and IE vibration ones from the IE data collected on the surface of concrete structures. Based on the test results, the following conclusions are reasoned out:

1. Delamination defects are differentiated from solid regions by dominant resonant responses at low frequencies (less than 6 kHz) and the amplitude spectrum at IE frequency corresponding to the slab depth. By using both modes of vibration, we can locate and size delamination defects in an efficient manner, as verified by experimental tests shown in this study.
2. A significant benefit of this approach is that the combined images include all the spectra in the predefined frequency range and also at the IE frequency. Thus, the inspectors are not required to know the frequency range with respect to the dynamic behavior of the delamination.
3. This approach can provide valuable results for field applications in detecting near-surface defects with various shapes, depths, and contact or boundary conditions in them.

Acknowledgements

This work was supported by the Incheon National University Research Grant in 2013.

References

Buyukozturk, O. (1998). "Imaging of concrete structures." NDT & E *International Journal*, Vol. 31, pp. 233-243, DOI: 10.1016/S0963-8695(98)00012-7, DOI: 10.1016/S0963-8695(98)00012-7, DOI: 10.1016/S0963-8695(98)00012-7.

Fuchs, P. and Washer, G. (2004). "Infrared thermographic bridge deck inspection on the Poplar street bridge." *in St. Louis MO, Proc., 6th Structural Materials Technology Conf.*, ASNT Publishing, Columbus OH.

Gannon, E. J. and Cady, P. D. (1992). *Condition Evaluation of Concrete Bridges Relative to Reinforcement Corrosion*, Vol. 1: State of the Art of Existing Methods (Report No. SHRP-S/FR-92-103), Strategic Highway Research Program, Washington DC.

Hime, W. and Erlin, B. (1987). "Some chemical and physical aspects of phenomena associated with chloride-induced corrosion." *Corrosion, Concrete, and Chlorides – Steel Corrosion in Concrete : Causes and Restraints*, SP-102, ACI, Detroit, MI, pp.1-12

Huston, D., Gucunski, N., Maher, A., Cui, A. J., Burns, J. D., and Jalinoos, D. F. (2007). "Bridge deck condition assessment with electromagnetic, acoustic and automated methods." *In: Sixth international workshop on structural health monitoring*, Stanford, CA, USA.

Johnson, K. L. (1985). *Contact mechanics*, Cambridge University Press.

Liu, P. L. and Yiu, C. Y. (2002). "Imaging of concrete defects using elastic wave tests." *the Far-East conference on nondestructive testing*, Tokyo, Japan.

Moore, M., Phares, B. Graybeal, B., Rolander, D., and Washer, G. (2001). *Reliability of visual inspection for highway bridges Vol. I: Final report*, Technical Report FHWA-RD-01-020, US Department of Transportation Federal Highway Administration.

Oh, T., Kee, S., Popovics, J. S., Arndt, R. W., and Zhu, J. (2012). "Comparison of NDT methods for assessment of a concrete bridge deck." *ASCE Journal of Engineering Mechanics*, Vol. 139, pp. 305-314, DOI: 10.1061/%28ASCE%29EM.1943-7889.0000441.

Oh, T. and Popovics, J. S. (2015a), "Practical visualization of local vibration data collected over large concrete elements." *Computer-Aided Civil and Infrastructure Engineering*, Vol. 30, pp. 68-81, DOI: 10.1111/mice.12065/abstract.

Oh, T. and Popovics, J. S. (2015b). "Application of impact-resonance C-scan stack images to evaluate bridge deck condition." *ASCE Journal of Infrastructure Systems*, Vol. 21, No. 1, pp. 21-26, DOI: 10.1061/(ASCE)IS.1943-555X.0000216.

Oh, T., Popovics, J. S., Ham, S., and Shin, S. (2013b), "Improved interpretation of vibration responses from concrete delamination defects using air-coupled impact resonance tests." *ASCE Journal of Engineering Mechanics*, Vol. 139, pp. 315-324, DOI: 10.1061/(ASCE)EM.1943-7889.0000491.

Oh, T., Popovics, J. S., and Sim, S. (2013a). "Analysis of vibration for regions above rectangular delamination defects in solids," *Journal of Sound and Vibration*, Vol. 332, pp. 1766-1776, DOI: 10.1016/j.jsv.2012.11.003.

Sansalone, M. J. and Streett, W. B. (1997), *Impact-echo : Nondestructive evaluation for concrete and masonry*, Bullbirer Press, Ithaca, N.Y.

Schubert, F., Wiggenhauser, H., and Lausch, R.(2004). "On the accuracy of thickness measurements in impact-echo testing of finite concrete specimens-numerical and experimental results." *Ultrasonics*, Vol. 42, pp. 897-901, DOI: 10.1016/j.ultras.2004.01.076.

Zhu, J. and Popovics, J. S. (2001). "Non-contact detection of surface waves in concrete using an air-coupled sensor." *in Review of Progress in Quantitative Nondestructive Evaluation*, 20B, edited by D.O. Thomson and D.E. Chimenti, AIP Conference Proceedings Vol. 615, American Institute of Physics, Melville,N.Y., pp. 1261-1268, DOI: 10.1063/1.1472940.

Zhu, J. and Popovics, J. S. (2007) "Imaging concrete structures using air-coupled impact-echo." *ASCE Journal of Engineering Mechanics*, Vol. 133, pp. 628-640, DOI: 10.1061/(ASCE)0733-9399(2007)133:6(628).